Rapidity Dependent Net-proton Yields in Au+Au at $\sqrt{s_{NN}} = 200$ GeV

J.H. Lee[a] for the BRAHMS Collaboration

[a]Physics Department
Brookhaven National Laboratory, Upton NY 11973

Net-proton yields $[N(p)-N(\bar{p})]$ have been measured by the BRAHMS collaboration at several rapidities $(0 \leq y_p \leq 3)$ in central Au+Au collisions at $\sqrt{s_{NN}} = 200$ GeV. The data exhibit an approximately constant rapidity density of net-protons within $|y| \lesssim 1$ which increases significantly toward $y{\sim}3$.

One of the primary goals of the Relativistic Heavy Ion Collider (RHIC) is to create and explore a highly excited baryon-poor region in heavy-ion collisions at extremely high energy. Contrary to the AGS [1] and SPS [2] energy regime where a large fraction of the initial baryons are piled up near mid-rapidity, at RHIC it has been conjectured that the nuclei pass through each other without much stopping. A central plateau may be created with approximately constant production of particles per unit of rapidity due to the breaking of color strings [3–5]. The degree of "transparency" of the plateau depends on the dynamics of the baryon number transport which itself depends on the early phases of the collision. Theoretical models predict different net-baryon (baryon − anti-baryon) density distributions based mainly on different assumptions about the initial conditions. In order to discriminate among the available models, measurements of the rapidity dependence of the net-baryon density are necessary.

The BRAHMS experiment at RHIC measures identified charged hadrons over a broad range of rapidity and transverse momentum with two movable spectrometers: the Mid-rapidity Spectrometer (MRS) and the Forward Spectrometer (FS) [6]. The data set used for this analysis were collected at a few selected rapidities: $y{\sim}0$ and $\sim$0.8 using the MRS, and $\sim$2.9 from the FS. Only the 0-10% most central events [4] were included in the analysis. Proton and anti-proton identification was done using a Time-of-Flight counter for MRS, and a Ring Image Cherenkov detector in the FS with momenta provided by multiple tracking detectors consisting of Time Projection Chambers and Drift Chambers and bending magnets [5,7,8]. Corrections have been applied to the reconstructed data to account for tracking inefficiencies and hadronic interactions. The geometrical acceptance factors are obtained from Monte-Carlo simulations. The spectra have not been corrected for protons and anti-protons from weak decays of Hyperons (Λ, Σ, *etc*).

The net-proton yield is defined as the number of non-pair-produced protons, which can be calculated as $N(p)-N(\bar{p})$. Figure 1 shows the p and $\bar{p}$ spectra for 0-10% central events. We fit the spectra with an m_T exponential function ($e^{-(m_T-m_p)/T}$) to extract the slopes and yields. The measured yields are $\sim$ 75% of extrapolated dN/dy at $y = 0$ and $\sim$ 40%

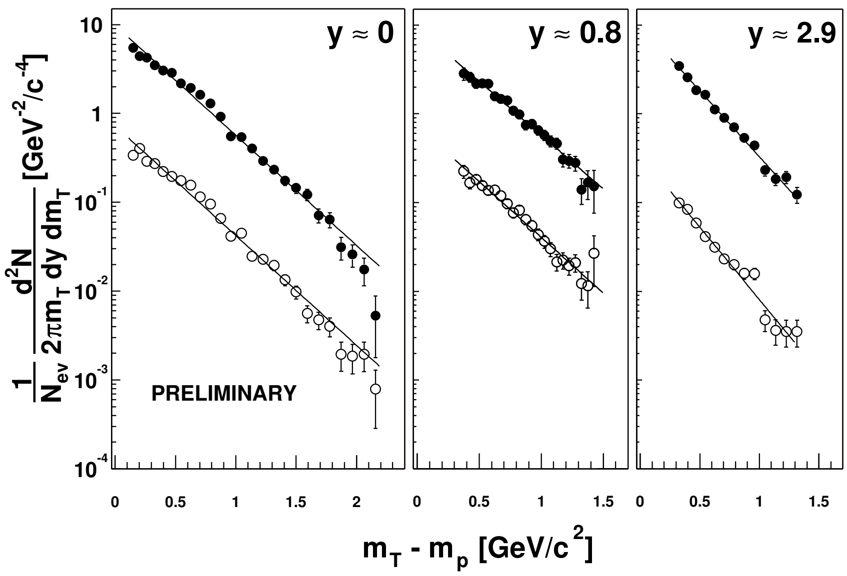

Figure 1. The m_T spectra for proton(•) and anti-proton(○) for central events (0-10%) at y∼0, 0.8, and 2.9. The proton spectra are shown at the correct scale, the anti-proton spectra are divided by a factor of 10 for clarity. Statistical error bars are shown or smaller than the symbol size. Solid lines represent exponential fits to the data.

Table 1
Inverse slope parameter (T) and dN/dy with statistical errors.

y	T_p (χ^2/DOF)	$T_{\bar{p}}$ (χ^2/DOF)	$T_{p-\bar{p}}$ (χ^2/DOF)	N_p	$N_{\bar{p}}$	$N_{p-\bar{p}}$
0	351±4 (91/23)	361±22 (73/23)	367±22 (20/23)	27.9±0.5	20.6±0.5	7.1±0.7
0.8	358±13 (15/20)	346±14 (15/20)	402±77 (11/20)	27.3±1.2	20.5±1.0	6.9±1.3
2.9	292±7 (15/10)	266±7 (16/10)	301±12 (9/10)	22.7±0.6	7.0±0.3	15.8±0.6

at the other rapidities, respectively. The inverse slope parameter (T) and dN/dy of the measurements are tabulated in Table 1. While data show approximately constant T and dN/dy values for p and $\bar{p}$ at y=0 and y=0.8, T and dN/dy for $\bar{p}$ decrease significantly at y∼2.9. We have used different functions to fit the mid-rapidity spectra. A fit with two-exponentials results in yields that are smaller by 8%, while a Boltzmann function ($m_T e^{-(m_T-m_p)/T}$) gives similar results as for an exponential. The major contribution to the systematic errors is from extrapolation to the low momentum region. Other main sources for the systematic errors are from uncertainties in estimating background contribution and track reconstruction efficiencies. Systematic errors for the values of net-protons are estimated to be ±15% for $y < 1$ and ±20% at y∼2.9. The net-proton yield at y∼0 is 7.1 ± 0.7(stat.)±1.1(sys.) and $15.8 \pm 0.6 \pm 3.5$ at y∼2.9.

We estimate that Λ feed-down corrections decrease the yields by 17.5% if it is assumed $N(\Lambda) = 0.9N(p)$ and $N(\bar{\Lambda}) = 0.95N(\bar{p})$ [9]. For y∼2.9, if we scale $N(\Lambda)_{y=0}$ by the ratio calculated from HIJING [11], $N(\Lambda)_{y=3}/N(\Lambda)_{y=0} \sim 0.7$. This results in a decrease of the

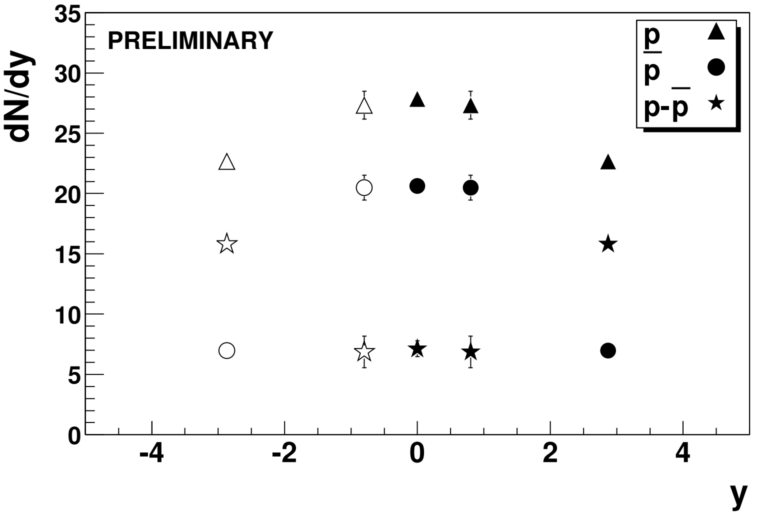

Figure 2. The rapidity densities (dN/dy) for p, $\bar{p}$ and $p-\bar{p}$ for central collisions (0-10%). Closed symbols refer to the measured points, and open symbols are values obtained by reflecting the measured data about mid-rapidity. The errors are statistical only.

net-proton yield by 20%. At y~0 this implies a net-baryon density of ~16 assuming that $N(p) = N(n)$ and $N(\text{net-}\Lambda)$=0.9N(net-proton). This is a dramatic decrease in the net-proton yield compared to SPS energies, dN/dy~27-32 [2] [10], indicating that substantial transparency has been achieved in these collisions. The rapidity dependence of the yield exhibits a boost-invariant behavior of the rapidity plateau for $|y| \lesssim 1$.

Comparisons of the measured net-proton yields with predictions from theoretical models are shown in Fig. 3. Models tested here are the ones using initial conditions based on pQCD and string dynamics which have been extensively compared with other measurements at RHIC: HIJING [11], HIJING/B [12], and AMPT [13]. The HIJING/B is a model based on HIJING with a baryon-junction mechanism implemented, which leads to more baryon stopping than HIJING. A MultiPhase Transport Model, AMPT, also takes the initial conditions from HIJING, but includes re-scattering processes with some of the model parameters tuned to the heavy-ion data from SPS. The measurement and the models are in reasonable agreement within systematic errors at the near mid-rapidity, while HIJING somewhat underestimate the stopping at the forward region. The AMPT model is also able to account for the general trend of the rapidity-dependent $N(\bar{p})/N(p)$ ratios [5] and the multiplicity distributions of charged particles [4] for the central collisions. It suggests that re-scattering plays a significant role in the dynamics of hadron distributions at RHIC energy. The microscopic transport model UrQMD [14] (not shown in Fig. 3), which reproduces many observed features at SPS energies predicts much higher stopping ($dN/dy|_{p-\bar{p}}$~12.5) at y=0.

In summary, we have presented first measurements of net-proton yields measured by BRAHMS collaboration at central and forward rapidities in central Au+Au collisions at $\sqrt{s_{NN}}$ = 200 GeV. The net-proton yields indicate that at RHIC we observe a boost-invariant rapidity plateau with a low net-baryon density in a narrow rapidity range of $|y| \lesssim 1$. It is estimated that the contribution from baryon-number transport to the total yield of the baryons at mid-rapidity decreases (~4−5 times) dramatically from SPS energy to RHIC energy. These results provide unique challenges and constraints to the theoretical models for baryon transport mechanism and initial conditions in nucleus-nucleus collisions

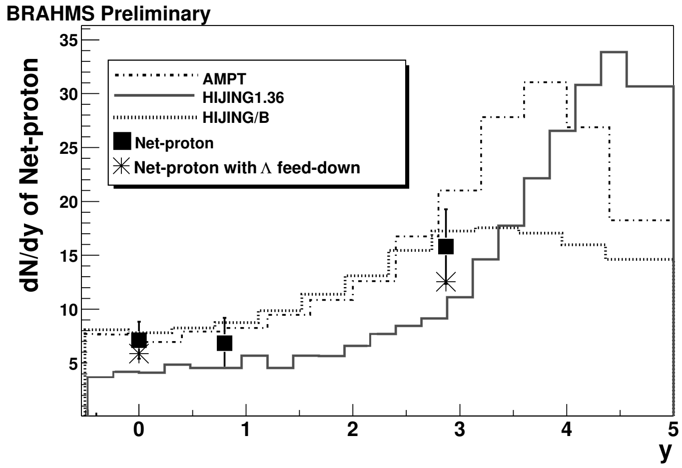

Figure 3. Net-proton distributions compared with theoretical models described in text. The errors include both statistical and systematic uncertainty. Net-proton yields with Λ feed-down corrections are shown at y=0 and 2.9.

at RHIC energy.

REFERENCES

1. E866 Collaboration, L. Ahle *et al.*, Phys. Rev. **C57** (1998) R466
2. NA49 Collaboration, H. Appelshaüser Phys. Rev. Lett. **82** (1999) 2471
3. J.D. Bjorken, Phys. Rev. **D27** (1983) 140
4. BRAHMS Collaboration, I.G. Bearden *et al.*, Phys. Rev. Lett. **88** (2002) 202301
5. BRAHMS Collaboration, Submitted to Phys. Rev. Lett., nucl-ex/0207006 (2002)
6. BRAHMS Collaboration, To be published in Nucl. Instrum. Meth.
7. D. Ouerdane (BRAHMS Collaboration), these proceedings.
8. I.G. Bearden (BRAHMS Collaboration), these proceedings.
9. PHENIX Collaboration, K. Adcox *et al.* Phys. Rev. Lett. **89** (2002) 092302
10. NA44 Collaboration, I. Bearden *et al.* Phys. Rev. **C66** 044907 (2002)
11. X.N. Wang and M. Gyulassy, Phys. Rev. **D44** (1991) 3501
12. S.E. Vance, M. Gyulassy, and X.N. Wang, Nucl.Phys. **A638** (1998) 395c
13. B. Zhang *et al.*, Phys. Rev. **C61** (2000) 067901
14. M.J. Bleicher *et al.*, Phys. Rev. **C62** (2000) 24904